Terahertz Imaging on Subcutaneous Tissues and Liver Inflamed by Liver Cancer Cells

C. H. Zhang [1, 4], G. F. Zhao [2], B. B. Jin [1*], Y. Y. Hou [2*], H. H. Jia [3], J. Chen [1] and P. H. Wu [1*]

[1] Research Institute of Superconductor Electronics (RISE), School of Electronic Science and Engineering, Nanjing University, Nanjing 210093, China

[2] Immunology and Reproductive Biology Lab, Medical School & State Key Laboratory of Pharmaceutical Biotechnology, Nanjing University, Nanjing, 210093, China

[3] Currently National University of Defense Technology, Changsha, 410008, China

[4] Institute of Laser Engineering, Osaka University, 2-6 Yamadaoka, Suita, Osaka 565-0871, Japan

[*1] Email: bbjin@nju.edu.cn, [*2] yayihou@nju.edu.cn & [*1] phwu@nju.edu.cn

Abstract: Terahertz (THz) imaging has a number of potential applications in medical imaging and diagnosis. Here, we demonstrate the THz images on the diseased and the corresponding normal tissues from 14 samples. The liver cancer cells are planted by subcutaneous injection into BALB/c which share high degree homology with human. Subcutaneous tumors and nearby normal tissues as well as the inflamed livers and normal liver tissues are achieved after 7 days, 14 days and 21 days injection. Terahertz time-domain spectroscopy (TDS) is used to image these tissues. We have found that at certain frequency range, most tumors and serious inflamed livers have lower absorption than normal tissues, which mean THz imaging could obviously distinguish the tumors and normal tissues, serious inflamed and normal livers, but could not obviously distinguish the grade of tumors and inflammation.

Keywords: THz imaging, biological tissue, absorption coefficient

1. Introduction

Liver cancer is a global health problem, representing the third cause of death for cancer and the fifth most common cancer worldwide [1-2]. It shows high prevalence in Asia and Africa [3].In China, especially in some rural area, its mortality rate is only less than gastric cancer. However, current diagnostic modalities, of ultrasound and α-fetoprotein, are expensive and lack sensitivity in tumor detection [4]. Once the symptoms of liver cancer appear in some people, it's generally too late to miss the best time of treatment. Since early diagnosis is integral to improved survival rate, it is important to study physical properties of the diseased tissues to find the possible ways for early diagnosis of liver cancer.

Terahertz (THz, 1 *THz*=10^{12} *Hz*) wave lies between the microwave and infrared regions of the electromagnetic spectrum and is typically defined as 0.1 to 10 *THz*. Due to its high penetration and low photon energy for biological tissues, it is of great importance on nondestructive biomedical and biological imaging that utilizes this radiation [5-13]. With the THz time domain spectroscopy (TDS), the THz imaging of basal cell carcinoma, a form of skin cancer, *ex vivo* in

the laboratory[14] and *in vivo* [15-17] as well as histo-pathological samples are shown. The strong contrasts have been revealed for different tissues [18]. Besides, the TDS imaging is used to map out tumor margins on the excised human breast tissue to give a good correlation between the area and shape of tumor deduced from histology [12]. These results encourage us to study other kinds of tumors with the THz imaging techniques.

Laboratory mice are commonly used for a variety of medical research purposes because they share a high degree of homology with human. At the same time, they are cheap and calm as well as easily handled and maintained in laboratory. In this paper, we planted liver cancer cells into BLAB/c by subcutaneous injection. Then, the parts of the diseased subcutaneous tumors and livers as well as the normal tissues nearby were excised at the 7th, 14th and 21st days, respectively. These diseased tissues with different grades and the corresponding normal tissues are imaged by TDS to study the differences. We hope to find the differences from the TDS images and further to find the physical reasons of these differences. Consequently, this TDS imaging technique is expected to advance the THz imaging research of biological tissues, and help the diagnosis of tumors.

2. Sample preparations

Tens of BALB/c mice (5-6 weeks old) were divided randomly into three groups, $100 \mu L$ H22 (liver cancer cell) suspension (10^7 *cells/mL*) was injected subcutaneously into the flank of BALB/c mice. After liver cancer cells were planted into the mice, subcutaneous tumors were obvious several days later. Simultaneously the tumor cells in the course metastasized to other organs with the development and malignancy aggravation of tumor through lymph nodes pathway. After 7, 14 and, 21 days, respectively, subcutaneous tumors, nearby normal tissues and livers were excised from each mouse. The livers from normal BALB/c were also excised as contrastive ones. On the surface, the livers from cancer-bearing mice had no difference with these from normal mice. Each diseased tissue was routinely divided into four parts, and the two of them were taken for the experiments. The one was stained with HE (Hematoxylin and Eosin) for histological examination, and other one was prepared for TDS imaging. Here, the samples for TDS imaging were two kinds: one was livers, and the other was subcutaneous tumors. Each sample consists of two parts: diseased tissues and corresponding normal ones for contrast. All the samples were dehydrated with alcohol, wax-mounted and cut into slices. The size of slice is about 26 *mm*×20 *mm*×1.5 *mm*.

3. Experimental procedure

In this study, all measurements are completed with a transmitted TDS imaging system (TPI Image 1000, TeraView Ltd, UK). A mode-locked Ti: sapphire laser by the Coherent company produced optical pulses with a time width less than 100 *fs* and a center wavelength of 800 *nm* at a

repetition rate of 82 *MHz*. Laser gated photo-conductive semiconductor antenna are used as the THz emitter and detector, and the available frequency range is about from 0.2 to 4 *THz*. THz beam is placed in a closed box where air is removed by vacuum pump and the humidity could be below 3% RH. THz scanning step is 0.5 *mm*, and each image consists of about 1600 *pixels*. As for 5 *times* averaged scanning, it took about 10 *minutes* for each sample.

4. Results

Figure 1 shows the photograph of five liver samples, each including the inflamed (left) and normal (right) liver tissues. Figure 2 shows the micrograph of histology. The samples were divided into three groups according to the histology results. From the histology results, the inflammation of liver 1# was serious. There were a large number of inflammatory cells infiltrating in the sample. The tissue structure was loose so the cell was deformed and the boundary was obscure. Sample 7# was a medium inflammation liver tissue. Focal cytomorphosis and infiltration of inflammatory cells was its main feature. Liver 4#, 8# and 13# had slight inflammation. They all had almost integrated structure and only small amounts of infiltrating inflammatory cells. These five samples were divided into 3 groups according to the grade of inflammation, as showed in table 1.
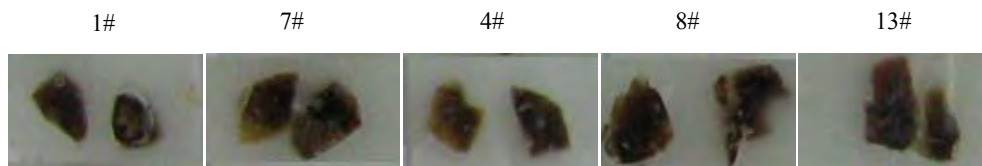
Fig. 1 Photograph of the five liver samples, the left and right parts were the inflamed and normal tissues, respectively.
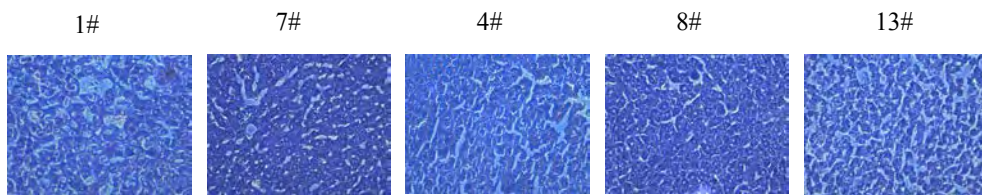
Fig. 2 Micrograph of HE staining tissues of inflamed livers

Tab. 1 The grade of all the liver samples

	Samples	Micrograph of HE staining tissues
Group a	1#	Serious inflammation
Group b	7#	Medium inflammation
Group c	4#, 8#, 13#	Slight inflammation

The images of THz absorption coefficient of each sample at five frequencies were illustrated in Fig. 3 [19-22]. The absorption coefficient of the normal tissues is larger than that of the inflamed

tissues, and the absorption increased with the frequency increasing. At low frequency, the absorption of all the samples is only a little larger than the wax, and the contrast of THz imaging is not good. While at high frequency, for example at about 1.70 *THz*, the absorption reached the highest, the difference between the normal and inflamed tissues also reached the largest, and the contrast of THz imaging was much better. If frequency was higher, the measured THz signal was at noise level, and SNR was very poor such as the image at 2.69 *THz*. The absorption of inflamed liver 1 was obviously much lower than corresponding normal liver, but the difference of the other four liver samples was not obvious. Therefore, TDS imaging could only distinguish serious inflamed livers.
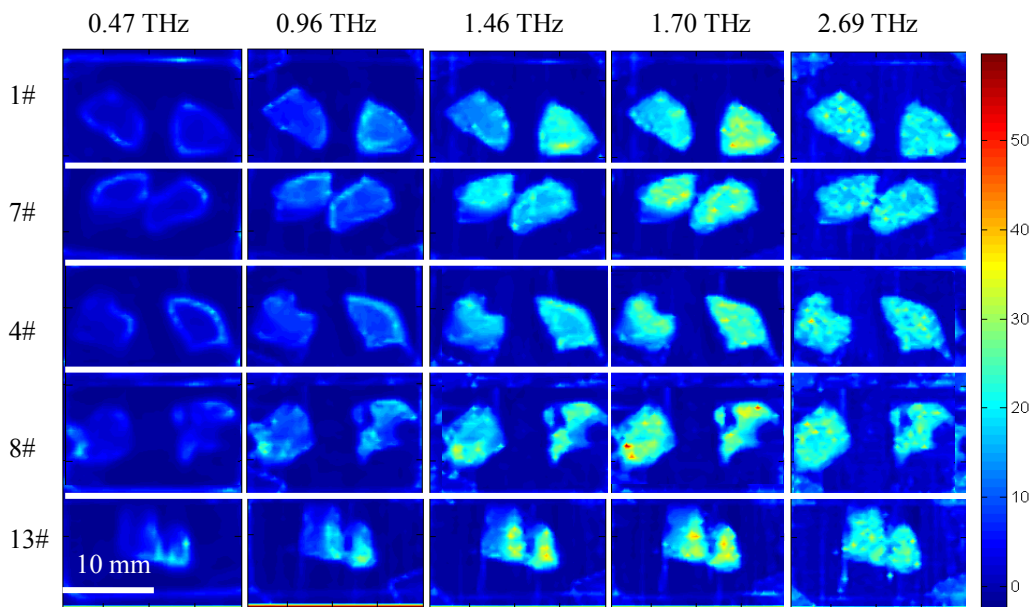
Fig. 3 THz absorption imaging of five liver samples
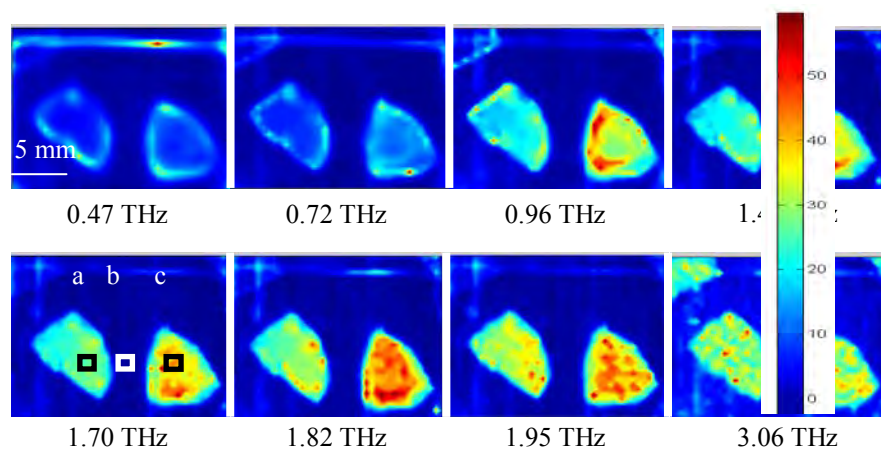
Fig. 4 THz absorption imaging of liver 1# at several frequencies
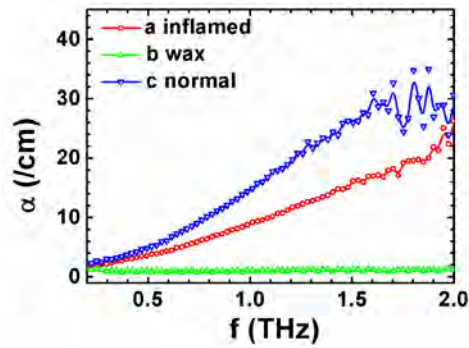
Fig. 5 Mean absorption of a,b,c areas.   Fig. 6 *Tα (ω)* curves of five liver samples
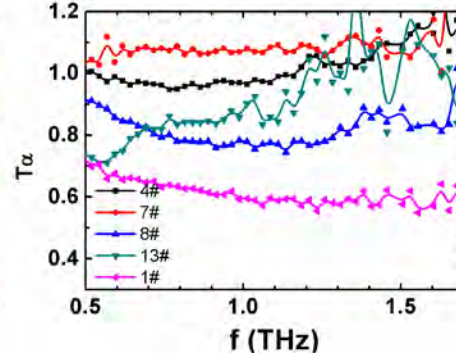
Figure 4 shows the THz absorption imaging of liver 1# at more frequency points. It can be easily found that the inflamed and normal tissues could be obviously distinguished at wide THz ranges. Figure 5 shows the mean absorption coefficient as a function of frequency, at areas marked with a, b and c, which represents inflamed liver, wax and normal liver, respectively. The absorption of wax was very small, which could be thought to be transparent. The absorption coefficient of inflamed liver was much lower than that of the normal ones, and both of them increased with the frequency. This behavior means the increasing of the working frequencies would lead to the improved contrast of the image. Above 2 *THz*, The signals are below the noise level, and are not displayed.

To describe better the measured data, we defined one image parameter as:

$$T\alpha(\omega) = \frac{\alpha_{diseased}(\omega)}{\alpha_{normal}(\omega)}$$

(1)

Where $\alpha_{diseased}(\omega)$ and $\alpha_{normal}(\omega)$ are the absorption coefficients of diseased and normal tissues, respectively. The parameter of $T\alpha(\omega)$ indicated the difference between diseased and normal tissues, and if $T\alpha(\omega)$ was far from 1, and the contrast of THz imaging was very high. Fig.6 shows the $T\alpha(\omega)$ curve of five liver samples. The parameter of $T\alpha(\omega)$ of liver1 was less than 1, and decreased with frequencies. It was 0.8 at 0.3 *THz* and reached 0.6 at about 1.7 *THz*. So the contrast of THz imaging at about 1.7 *THz* arrived at the best. While from 1 to 1.7 *THz*, the parameter of $T\alpha(\omega)$ remained almost the same, which means THz imaging is good in the frequencies from 1 to 1.7 *THz*. But for the other four liver samples, the parameter of $T\alpha(\omega)$ was almost about 1, and the contrast of corresponding THz imaging was very poor, so the THz imaging could not distinguish these non-seriously inflamed samples.

The subcutaneous tumor samples were studied by the same TDS imaging and histology. Figure 6 shows the photograph of the 12 samples, and the left part was the tumor while the right part was the normal tissues of each sample. Figure 7 shows the results of micrograph of HE staining tissues of all the 12 tumors. Samples were divided into 5 groups according to the grade of tumor histology, showed in table 2. The samples of group A had large areas of necrosis. Its cellular structure and profile vanished and cell nucleus was dissolved. Focal necrosis, even lamellar

necrosis, was found in samples of group B and most of the tissue structure was not integrated. The samples for group C and D were focal necrotic tumor tissues, but fresh granuloma and tumor fibrosis were appearing in tissues of group D. Sample in Group E was going to necrosis. They had complete cellular structure but its cellular shape and nucleus started to change.
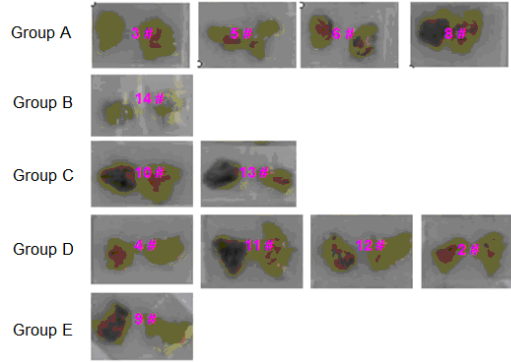
Fig. 7 Photograph of the subcutaneous tumor samples

(a) 0.96 *THz*   (b)1.7 *THz*
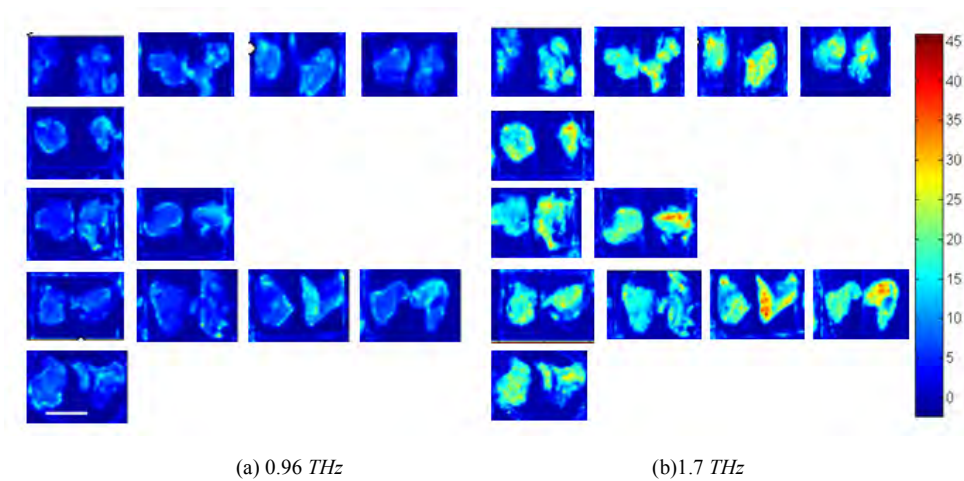
Fig. 8 THz absorption imaging at 0.96 *THz* and 1.7 *THz* of subcutaneous tumor samples

Tab. 2 Samples of subcutaneous tumor

	Samples	Micrograph of HE staining tissues
Group A	3#, 5#, 6#, 8#	Large areas of necrosis
Group B	14#	Focal necrosis to lamellar necrosis
Group C	10#, 13#	Focal necrosis
Group D	2#, 4#, 11#, 12#,	Focal necrosis, Granuloma, Tumor fibrosis
Group E	9#	Going to necrosis

The same procedure was also done to the subcutaneous tumor samples. Figure 8 shows the absorption imaging at 0.96 *THz* and 1.7 *THz*. The absorption of all the samples increased with increasing frequency and the absorptions of tumors were less than those of normal tissues. At low

frequency, as the absorptions of tumors and normal tissues were small, not much larger than the background wax, and their differences were also small, the contrast of THz imaging was of course not good, the tumors and normal tissues were not obviously distinguished. At high frequency, for example at about 1.7 *THz*, the difference of absorption was larger, they could be distinguished obviously, and the contrast of THz imaging was better. But the difference of absorption between these five grades of tumors was not observed, the grade of tumors could not be distinguished by THz imaging.
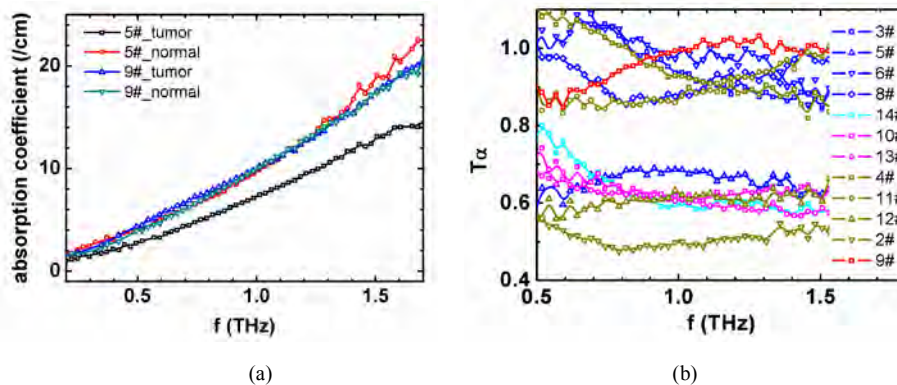
Fig. 9 (a) The absorption of tumor sample 5# and 9# (b) *Tα(ω)* curves of all the tumor samples, each color of curve mean each group

   The absorptions between different normal tissues were almost the same. Figure 9 (a) showed the absorption curve of sample 5# and 9#. The absorption coefficients increased with increasing frequencies, and the normal tissues from 5# and 9# had almost the same absorption. The tumor of sample 5# had obviously less absorption than normal one, but the tumor of sample 9# had almost the same absorption with normal one. Figure 9 (b) showed the Tα(ω) curve of all the subcutaneous tumor samples. The same color curve showed the same group samples, and different symbols showed different samples. All the values of Tα(ω) were almost less than one, and the values could be divided into two groups: one was about 0.6, and the tumors and normal tissues from these samples could be distinguished at THz imaging. The other was near one, which indicated the difference between tumor and normal tissues was very small. However, the contrast of THz imaging was bad, and the tumor and normal tissues could not be distinguished by the THz imaging. The results showed that THz imaging technology may be available at certain frequency range, and about half samples could be distinguished.

5. Discussions

   Although 21 mice were prepared, only 14 mice samples were successful. All the results could be summarized as: most histology results were proportional to the injection time. For THz imaging of liver samples, only the most seriously inflamed sample 1 could be distinguished. And for subcutaneous tumors, about 6 in 12 samples could be distinguished, and 4 samples were from

the group with short injection time. From these results, we can say that THz imaging technology may be useful for the early diagnosis of tumors.

From the results, it is also obvious that only half the image matches optical HE image, i.e., THz imaging can not identify all the diseased and normal tissues. This needs us to consider the precise source of the contrast in the THz imaging, which is still not clear so far. In our case, the scattering effect is negligible since the wavelengths are significantly larger than the structure in tissue. Moreover, all the samples in this paper were dehydrated with alcohol; the effect from water content to THz imaging could be neglected. The possible reason of the contrast comes from the difference of tissue density between diseased and normal tissues. Fig.5 shows the absorption coefficient is almost linear with frequency, which implies that the refractive index is a constant for each sample. As we know the refractive index of the tissue is related to the tissue density. The normal tissues had high tissue density and more closely cell-to-cell connection, while the cells of diseased tissues were necrotic and deformed, and its integrated cell morphology, even nucleus was lost. These changes made the loose structure and low density of tumor tissues. So, the absorption of the normal tissue is always higher than that of the diseased one, which is consistent with our experiments.

However, we found that the absorptions for about half of the all samples are very close to the normal issue, leading to the very low contrast. This may be caused by another thing that TDS imaging represents not only the structure but also the chemical constituents of the sample, for example, the cellular content and changed proteins. This is quite obvious from the optical images of HE staining tissues, which represents only the change of the structure of the tissues. In this case the mismatch between two methods is not strange. Due to its spectroscopic property, THz imaging can offer both structural and functional information in this frequency range [16-17].

The method in this paper also had some limitations. As the individuals of BALB/c had difference, the growth of tumors in the same group was either not completely same, and the cells maybe distort or shrink. The thickness of samples for histology and THz imaging was much different, the sample for histology was only several micrometers thick, while the sample for THz imaging was about more than 1 millimeter, and the surface of THz samples was not completely flat and smooth. All these factors may result in the difference between the histology and THz imaging. So some/further work should be done to improve the error of TDS system and sample making, which would make the THz imaging technology be more available and reliable in clinical examinations.

6. Conclusion

THz TDS imaging technology was used to study the subcutaneous tumors, inflamed liver and their corresponding normal tissues. The THz property of different grade of diseased samples was also studied. THz imaging was obtained based on the absorption coefficient. The results showed that at certain frequency range, subcutaneous tumors and inflamed livers had less absorption than

their corresponding normal tissues, so TDS imaging could be applied to distinguish the diseased and the normal tissues at a certain extent. Although the individuals of BALB/c had difference, the absorption of normal tissues from different samples was almost the same. The contrast of THz imaging was depended on the different sample and frequency. Therefore, TDS imaging technology may advance the imaging research of biological tissues, and help the diagnosis of tumors.

References and links

[1] S. Caldwell and S. H. Park, "The epidemiology of hepatocellular cancer: from the perspectives of public health problem to tumor biology", *J Gastroenterol* 44, 96-101 (2009).

[2] M. Roncalli, L. Terracciano, L. Di Tommaso, E. David, M. Colombo, Gipad, and Iap, "Liver precancerous lesions and hepatocellular carcinoma: The histology report", *Digest Liver Dis* 43, S361-S372 (2011).

[3] F. X. Bosch, J. Ribes, M. Diaz, and R. Cleries, "Primary liver cancer: Worldwide incidence and trends", *Gastroenterology* 127 (5), S5-S16 (2004).

[4] M. Patel, M. I. Shariff, N. G. Ladep, A. V. Thillainayagam, H. C. Thomas, S. A. Khan, and S. D. Taylor-Robinson, "Hepatocellular carcinoma: diagnostics and screening", *Journal of Evaluation in Clinical Practice* 01599 1365-2753 (2011).

[5] E. Pickwell and V. P. Wallace, "Biomedical applications of terahertz technology", *Journal of Physics D-Applied Physics 39* (17), R301-R310 (2006).

[6] A. J. Fitzgerald, V. P. Wallace, M. Jimenez-Linan, L. Bobrow, R. J. Pye, A. D. Purushotham, and D. D. Arnone, "Terahertz pulsed imaging of human breast tumors", *Radiology* 239 (2), 533-540 (2006).

[7] R. M. Woodward, V. P. Wallace, D. D. Arnone, E. H. Linfield, and M. Pepper, "Terahertz pulsed imaging of skin cancer in the time and frequency domain", *Journal of Biological Physics* 29 (2-3), 257-261 (2003).

[8] R. M. Woodward, B. E. Cole, V. P. Wallace, R. J. Pye, D. D. Arnone, E. H. Linfield, and M. Pepper, "Terahertz pulse imaging in reflection geometry of human skin cancer and skin tissue", *Physics in Medicine and Biology* 47 (21), 3853-3863 (2002).

[9] J. Nishizawa, T. Sasaki, K. Suto, T. Yamada, T. Tanabe, T. Tanno, T. Sawai, and Y. Miura, "THz imaging of nucleobases and cancerous tissue using a GaP THz-wave generator", *Optics Communications* 244 (1-6), 469-474 (2005).

[10] E. Pickwell, A. J. Fitzgerald, B. E. Cole, P. F. Taday, R. J. Pye, T. Ha, M. Pepper, and V. P. Wallace, "Simulating the response of terahertz radiation to basal cell carcinoma using ex vivo spectroscopy measurements", *Journal of Biomedical Optics* 10 (6) (2005).

[11] E. Pickwell, B. E. Cole, A. J. Fitzgerald, V. P. Wallace, and M. Pepper, "Simulation of terahertz pulse propagation in biological systems", *Applied Physics Letters* 84 (12), 2190-2192 (2004).

[12] K. J. Siebert, T. Loffler, H. Quast, M. Thomson, T. Bauer, R. Leonhardt, S. Czasch, and H. G. Roskos, "All-optoelectronic continuous wave THz imaging for biomedical applications", *Physics in Medicine and Biology* 47 (21), 3743-3748 (2002).

[13] S. Y. Huang, Y. X. J. Wang, D. K. Wyeung, A. T. Ahuja, Y. T. Zhang, and E. Pickwell-MacPherson, "Tissue characterization using terahertz pulsed imaging in reflection geometry", *Physics in Medicine and Biology* 54 (1), 149-160 (2009).

[14] R. M. Woodward, V. P. Wallace, R. J. Pye, B. E. Cole, D. D. Arnone, E. H. Linfield, and M. Pepper, "Terahertz pulse imaging of ex vivo basal cell carcinoma", *Journal of Investigative Dermatology* 120 (1), 72-78 (2003).

[15] V. P. Wallace, P. F. Taday, A. J. Fitzgerald, R. M. Woodward, J. Cluff, R. J. Pye, and D. D. Arnone, "Terahertz pulsed imaging and spectroscopy for biomedical and pharmaceutical applications", *Faraday Discussions* 126, 255-263 (2004).

[16] V. P. Wallace, A. J. Fitzgerald, S. Shankar, N. Flanagan, R. Pye, J. Cluff, and D. D. Arnone, "Terahertz pulsed imaging of basal cell carcinoma ex vivo and in vivo", *British Journal of Dermatology* 151 (2), 424-432 (2004).

[17] E. Pickwell, B. E. Cole, A. J. Fitzgerald, M. Pepper, and V. P. Wallace, "In vivo study of human skin using pulsed terahertz radiation", *Physics in Medicine and Biology* 49 (9), 1595-1607 (2004).

[18] P. Knobloch, C. Schildknecht, T. Kleine-Ostmann, M. Koch, S. Hoffmann, M. Hofmann, E. Rehberg, M. Sperling, K. Donhuijsen, G. Hein, and K. Pierz, "Medical THz imaging: an investigation of histo-pathological samples", *Physics in Medicine and Biology* 47 (21), 3875-3884 (2002).

[19] Timothy D. Dorney, Richard G. Baraiuk, and Daniel. M. Mittleman, "Material parameter estimation with terahertz time domain spectroscopy", *J. Opt. Soc. Am. A* 18 (7), 1562-1571 (2001).

[20] Lionel; Duvillaret, Frédéric; Garet, and Jean-Louis Coutaz, "Highly precise determination of Optical Constants and sample thickness in Terahertz Time-Domain Spectroscopy", *Applied Optics* 38 (2), 409-415 (1999).

[21] Ioachim Pupeza, Rafal Wilk, and Martin Koch, "Highly accurate optical material parameter determination with THz time-domain spectroscopy", *Optics Express* 15 (7), 4335-4350 (2007).

[22] D. Grischkowsky, Søren Keiding, Martin van Exter, and Ch. Fattinger, "Far-infrared time-domain spectroscopy with terahertz beams of dielectrics and semiconductors", *J. Opt. Soc. Am.* B 7 (10), 2006-2015 (1990).